Food & Function

ROYAL SOCIETY OF CHEMISTRY

PAPER

View Article Online
View Journal | View Issue

Cite this: *Food Funct.*, 2023, **14**, 2416

Integration of transcriptomics and metabolomics to reveal the effect of ginsenoside Rg3 on allergic rhinitis in mice†

Jianming Liu,[a] Na Yang,[b] Xingcheng Yi,[c] Guoqiang Wang,[d] Cuizhu Wang,[e] Hongqiang Lin,[d] Liwei Sun,[a] Fang Wang*[d] and Dongdong Zhu *[a,f]

Increasing studies have demonstrated that ginsenoside Rg3 (Rg3) plays an important role in the prevention and treatment of various diseases, including allergic lower airway inflammation such as asthma. To investigate the role of Rg3 in allergic upper airway disease, the effect and therapeutic mechanism of Rg3 in allergic rhinitis (AR) were studied. Ovalbumin-induced AR model mice were intragastrically administered with Rg3. Nasal symptoms, levels of IgE, IL-4, IL-5, IL-13, SOD and MDA in serum, and histopathological analysis of nasal mucosa were used to evaluate the effect of Rg3 on ameliorating AR in mice. Moreover, nasal mucosa samples from the normal control group, AR model group and high dosage of Rg3 were collected to perform omics analysis. The differentially expressed genes and significantly changed metabolites were screened based on transcriptomics and metabolomics analyses, respectively. Integrative analysis was further performed to confirm the hub genes, metabolites and pathways. After Rg3 intervention, the nasal symptoms and inflammatory infiltration were effectively improved, the levels of IgE, IL-4, IL-5, IL-13 and MDA were significantly reduced, and the level of SOD was obviously increased. The results of the qRT-PCR assay complemented the transcriptomic findings. Integrated analysis showed that Rg3 played an anti-AR role mainly by regulating the interaction network, which was constructed by 12 genes, 8 metabolites and 4 pathways. Our findings suggested that Rg3 had a therapeutic effect on ovalbumin-induced AR in mice by inhibiting inflammation development and reducing oxidative stress. The present study could provide a potential natural agent for the treatment of AR.

Received 14th December 2022,
Accepted 20th January 2023

DOI: 10.1039/d2fo03885d

rsc.li/food-function

1. Introduction

Ginseng, a famous traditional Chinese medicine with ginsenosides as the main active ingredient, has been used clinically for more than 1500 years. Ginsenosides are the major bioactive components of ginseng. It has been reported that ginsenosides Rb1,[1] Rd,[2] Rg1,[3] Rg3,[4] Rh1[5] and Rh2[6] all could alleviate allergic airway inflammation. Among these compounds, Rg3 plays a prominent role in alleviating oxidative stress.[4] Moreover, it was proven that red ginseng has a better effect on improving allergic airway inflammation than ginseng.[7] Compared to ginseng, the content of Rg3 was obviously higher in red ginseng.[8,9] Therefore, Rg3 was selected to be used in our study. Ginsenoside Rg3 (Rg3), a rare saponin in ginseng, was reported to have pharmacological effects, such as anti-inflammatory, antioxidant, anticancer,[10] antiulcer,[11] neuroprotective,[12] anti-fatigue,[13] and anti-aging activities[14] and used for adjuvant therapy of rheumatoid arthritis.[15] Recently, there have also been some research reports on the role of Rg3 in the treatment of allergic lower airway diseases. For example, in inflammatory BEAS-2B cells, Rg3 could inhibit the expression of eotaxin, proinflammatory cytokines and ICAM-1. In asthmatic mice, eosinophil infiltration, oxidation reactions, airway inflammation and hyperresponsiveness were all significantly improved by intraperitoneal injection of Rg3.[4] In A549 cells and human asthmatic lung tissue, Rg3 showed good anti-inflammatory effects *via* the NF-κB pathway.[16] In addition, Rg3 could also inhibit mast cell-mediated allergic responses by reducing the release of histamine and proinflammatory cytokines through the MAPK/NF-κB and RIP2/caspase-1 pathways.[17]

[a]*Department of Otolaryngology Head and Neck Surgery, China-Japan Union Hospital of Jilin University, Changchun 130021, China. E-mail: zhudd@jlu.edu.cn*
[b]*Clinical Pharmacy Department, First Hospital of Jilin University, Changchun 130021, China*
[c]*Laboratory of Cancer Precision Medicine, First Hospital of Jilin University, Changchun 130061, China*
[d]*Department of Pathogen Biology, College of Basic Medical Sciences, Jilin University, Changchun 130021, China. E-mail: wf@jlu.edu.cn*
[e]*School of Pharmaceutical Sciences, Jilin University, Changchun 130021, China*
[f]*Jilin Provincial Key Laboratory of Precise Diagnosis and Treatment of Upper Airway Allergic Diseases, Changchun 130021, China*

† Electronic supplementary information (ESI) available. See DOI: https://doi.org/10.1039/d2fo03885d

Allergic upper airway disease, such as allergic rhinitis (AR), has been a common and significant global public health problem in recent decades. AR has been a subject of continuous concern for the WHO for a long time.[18] The pathogenesis of AR involves a number of intricate immune and inflammatory responses. For example, exposure to allergens or other substances can induce AR attacks caused by IgE-mediated reactions.[19] The major clinical symptoms are nasal itching, sneezing, rhinorrhea and nasal congestion. According to global treatment guidelines, the neurotropic and hormonal drugs currently used to treat AR include oral H-antihistamines, intranasal H-antihistamines, intranasal corticosteroids, leukotriene receptor antagonists and glucocorticoids alone or in combination.[20] However, there has been increasing concern about the associated undesirable side effects. Therefore, the search for a safer and more effective cure is still a key priority. Therefore, medical researchers have devoted themselves to the development of natural products in recent years such as Sargassum horneri,[21] vanillic acid[22] and *Rosa multiflora* Fructus water extract.[23] Among these, Bu-zhong-yi-qi-tang consisting of ginseng and other herbs plays an important role in AR treatment by improving nasal symptoms and inhibiting the levels of total serum IgE and IL-4-mediated inflammatory reactions involving COX-2 associated with oxidative stress and the expression of other mRNAs.[24] A randomized controlled trial in Korea showed that oral administration of red ginseng could improve rhinorrhea, nasal itching and eye itching and reduce total IgE and IL-4 levels in serum and eosinophil counts in nasal smears. It could be concluded that red ginseng showed good curative effects on AR patients.[25] The content of Rg3 in red ginseng is much higher than that in ginseng. However, there have been few reports about the effects of Rg3 in AR.

The multiomics approach, including transcriptomics and metabolomics, could more effectively help researchers in gaining a deeper understanding of the pathogenesis and therapeutic mechanisms of allergic airway diseases including AR and asthma.[26,27] Chinese herbal medicines and natural products taken orally or applied externally were recommended in Allergic Rhinitis and its Impact on Asthma (ARIA) guidelines and Chinese AR guidelines.[18] For instance, the potential nosogenesis and development processes of AR were explored based on metabolomics or transcriptomics.[28,29] The therapeutic mechanisms of paeoniflorin, a natural product, on allergic asthma were studied by the integration of metabolomics and transcriptomics.[30]

To explore the effect of Rg3 on AR, the ovalbumin (OVA)-induced AR model was established in mice in the current study. After intragastric administration of Rg3, transcriptomics and nontargeted metabolomics were used to identify differentially expressed genes (DEGs) and metabolites in nasal mucosa samples of AR mice and Rg3-treated AR mice, respectively. Subsequently, integrated analysis of transcriptomics and metabolomics was performed to obtain the key genes and metabolites to elucidate the therapeutic mechanisms of Rg3 in AR. This study could provide a potential natural agent for the treatment of AR.

2. Results

2.1. The effect of Rg3 on OVA-induced AR mice

2.1.1. Nasal symptoms. As shown in Fig. 1A and B, compared with the NC group, nasal symptoms such as sneezing and nasal rubbing in the OVA group were significantly increased ($p < 0.001$), which indicated that the OVA-induced model of AR was successfully established. Compared with the OVA group, AR mice treated with dexamethasone (DEX) or Rg3 significantly decreased the numbers of sneezing and nasal rubbing ($p < 0.05$, $p < 0.01$, $p < 0.001$). In addition, the intervention effects of Rg3 were dose dependent.

2.1.2. ELISA detection of IgE, inflammatory cytokine and oxidative stress levels. It was well known that the Th2-type cytokine-induced immune response was the key to the development of AR.[31] Consequently, ELISA was used to evaluate allergic airway inflammation in all groups (Fig. 1C–H). In serum, the levels of IgE, IL-5, IL-13 and IL-4 in the OVA group were at distinctly higher concentrations than those in the normal control (NC) group ($p < 0.001$). Compared with the OVA group, Rg3-H and DEX conspicuously attenuated the expression of IgE, IL-5, IL-13 and IL-4 ($p < 0.01$, $p < 0.001$). In addition, treatment of AR mice with Rg3-L and Rg3-M also significantly attenuated IL-13 or IL-4 compared with untreated AR mice ($p < 0.05$, $p < 0.01$).

Compared with the NC group, malondialdehyde (MDA) in the OVA group was significantly increased ($p < 0.001$), while superoxide dismutase (SOD) was significantly decreased ($p < 0.001$). Compared with the OVA group, SOD in the Rg3-H and DEX groups was obviously increased ($p < 0.01$), MDA in the Rg3-H and DEX groups was obviously decreased ($p < 0.001$), while SOD and MDA in the Rg3-L and Rg3-M groups showed no obvious difference. The results showed that Rg3-H could reduce oxidative damage in AR mice and enhance their antioxidant capacity.

2.1.3. Histopathological examination. To evaluate the effect of Rg3 on AR mice induced by OVA, the nasal mucosa was stained with H&E. The results showed that compared with NC group mice, the infiltration of inflammatory cells such as eosinophils in the OVA group mice increased. In contrast, compared with that in the OVA group, the inflammatory cell infiltration in the Rg3-H group and DEX group was significantly reduced (Fig. 1I).

2.2. Rg3 treatment alters the transcriptome in OVA-induced mice

Genes in nasal tissues of the NC, OVA and Rg3-H groups were obviously separated into different regions based on principal component analysis (PCA) (Fig. 2A). To identify the DEGs that changed significantly in the three groups, the DEseq2 algorithm was then performed on the transcriptome datasets of nasal mucosa. The Venn diagram was used to screen DEGs in the Rg3-H group with expression close to that in the NC group. As a result, a total of 115 genes were identified as DEGs that played a potentially important role in the treatment of AR with Rg3 (Fig. 2B). A total of 115 DEGs and their expression in the

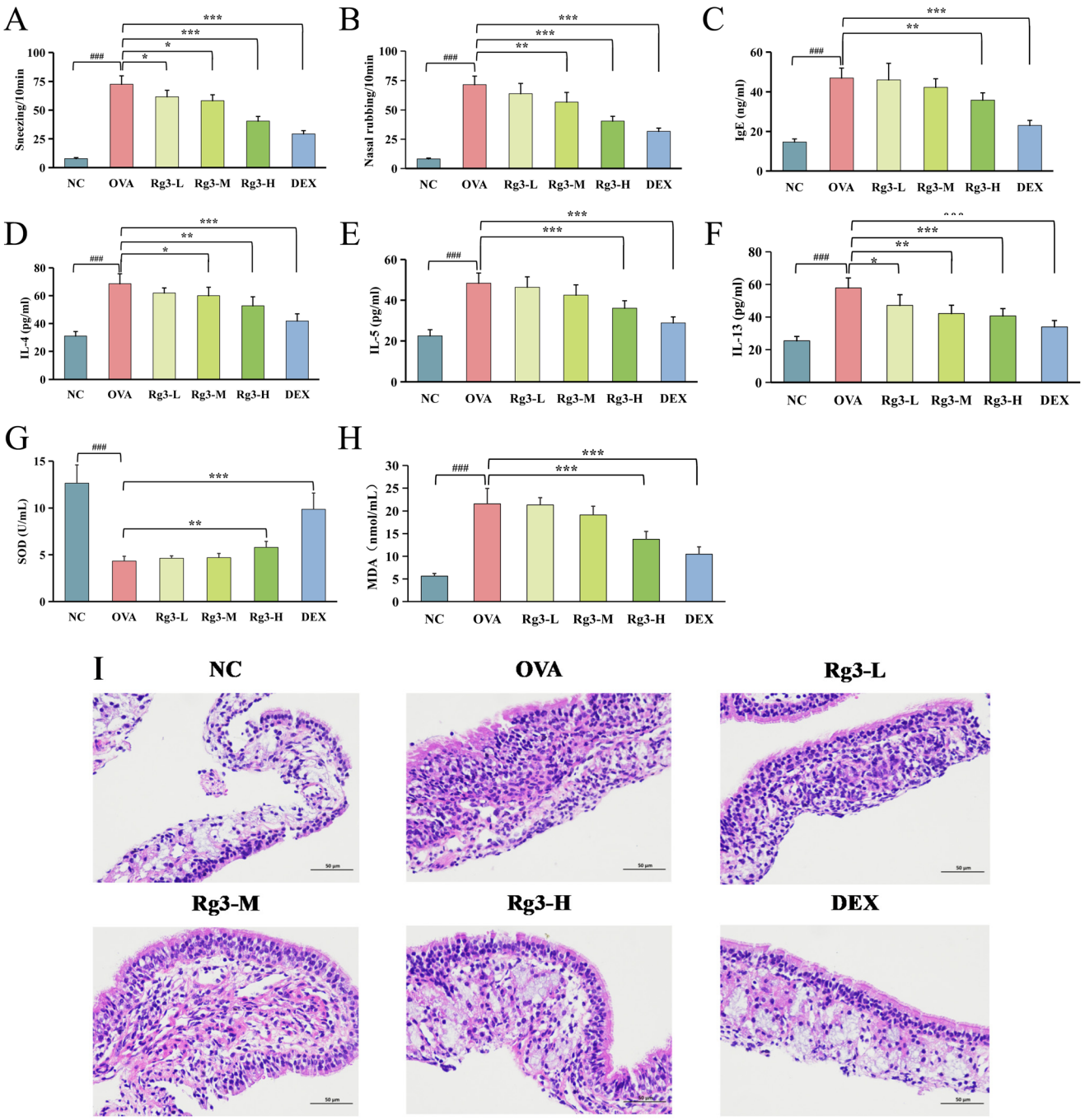

Fig. 1 The effect of Rg3 on AR mice. Frequency of sneezing (A) and nasal rubbing (B) in mice (n = 6). The levels of IgE (C), IL-4 (D), IL-5 (E), IL-13 (F), and SOD (G), and MDA (H) in the serum of mice (n = 6). (I) Images of hematoxylin and eosin (H&E) staining of the nasal mucosa (n = 6). Bars = 50 μm. Data are presented as mean ± SD. $^{###}p < 0.001$, $^{*}p < 0.05$, $^{**}p < 0.01$, $^{***}p < 0.001$.

three groups were visualized through a heatmap (Fig. 2C). In the heatmap, the region from blue to red represents an increasing abundance of DEGs.

2.3. Rg3 treatment alters metabolism in OVA-induced mice

Metabolomics analysis was also performed in the NC, OVA and Rg3-H groups. In the validation of UPLC-Q/TOF-MS, the RSDs of the peak intensity and RT in the system stability, precision, reproducibility and sample stability tests were all less than 3.0%. From the results, the established method exerted good reproducibility, precision and stability and could be used for analyzing the tested samples. As shown in the PCA score plots (Fig. 3A and B), the NC group, OVA group and Rg3-H group were clearly separated into different regions. The Rg3-H group

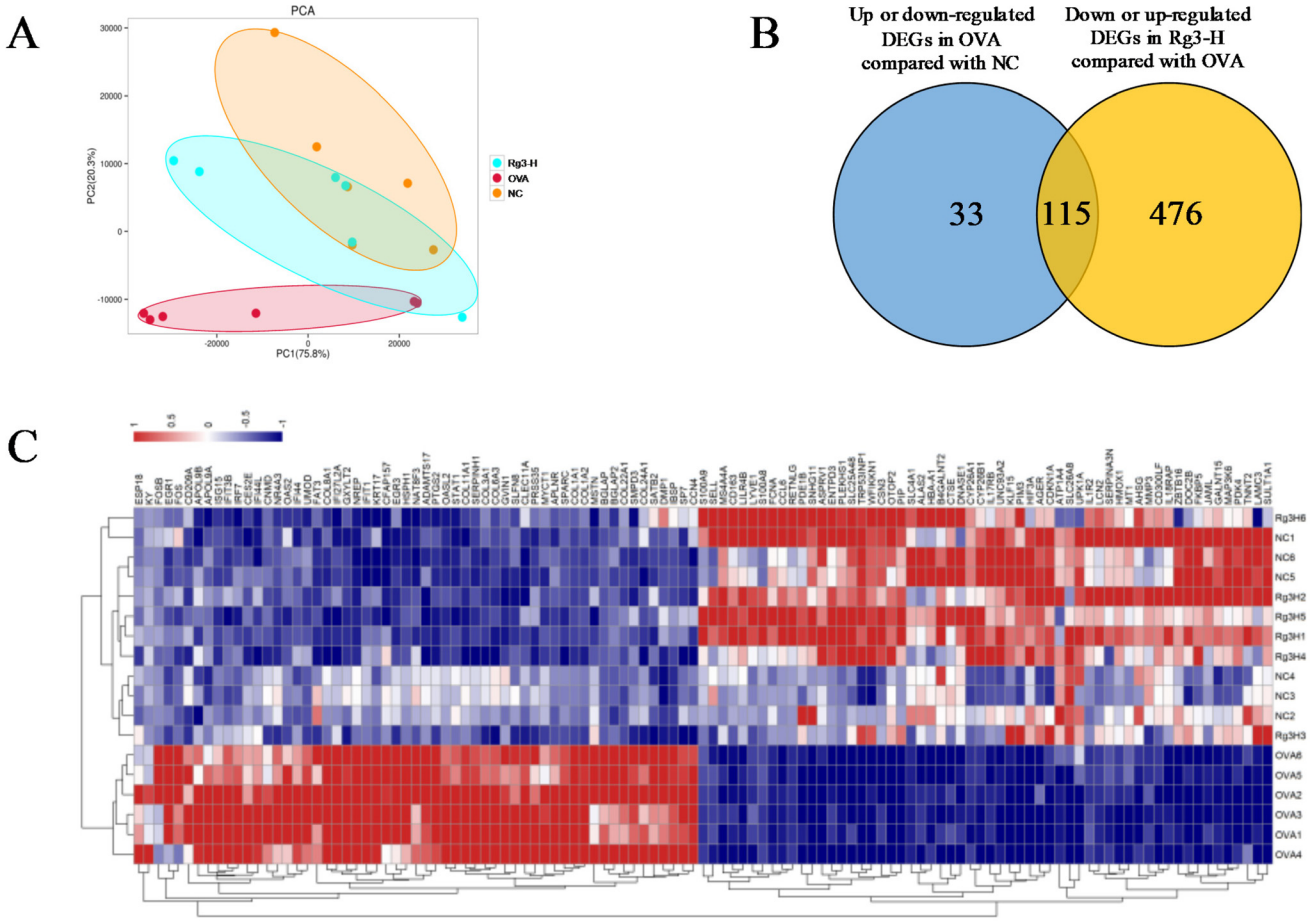

Fig. 2 Transcriptomic altered with Rg3 treatment in AR mice. (A) PCA analysis of DEGs in the nasal mucosa of NC, OVA and Rg3-H groups. (B) Venn diagram of DEGs. (C) Heatmap of the expression of 115 DEGs.

was located between the NC group and OVA group, indicating that Rg3 could improve metabolic disturbances in AR model mice.

Orthogonal projections to latent structures discriminant analysis (OPLS-DA) were then established (Fig. 3C and D) to obtain the maximum separation between the two groups. The OVA and Rg3-H samples were separated to the greatest extent with a satisfactory goodness of fit (R^2 = 0.9955 and Q^2 = 0.7769 in ESI^+; R^2 = 0.9996 and Q^2 = 0.8922 in ESI^-).

Additionally, in the permutation test, all Q^2-values to the left were lower than the original points to the right, suggesting the validity of the original models (Fig. 3E and F). The generated volcanic plots (Fig. 3G and H) were used to screen the differentiated metabolites. A total of 8 differential metabolites between the OVA group and Rg3-H group were identified as potential biomarkers and were marked in blue. Then, predictive receiver operating characteristic (ROC) curves were generated by using these potential biomarkers (Fig. 3I). All the areas under the curves (AUCs) of the biomarkers were greater than 0.80, indicating that these 8 metabolites could be considered potential markers, which contributed to the effect of Rg3-H on AR treatment (Tables 1 and 2).

2.4. Integrative analysis of metabolomic and transcriptomic data

2.4.1. Canonical correlation analysis. Canonical correlation analysis (CCA) could show the correlation between two groups of data as a whole through the comprehensive analysis of variables.[32] In the present study, a total of 115 DEGs were converted using the R package and 8 differential metabolites were analyzed by CCA. The total explained variation of the explanatory variable matrix (metabolites) to the response variable matrix (genes) was 94.0% (CCA1 + CCA2), indicating that the analysis had high reliability. Top 20 genes and 8 metabolites were screened, which might play an important role in Rg3 treatment of AR mice (Fig. 4A). The light blue and yellow dots represent the Rg3-H group and OVA group, respectively. The dark blue dots and red arrows represent the top 20 genes and 8 metabolites after screening, respectively. The top 20 genes were as follows: CDKN1A, COL1A1, COL1A2, COL3A1, CSN3, CYP26B1, DNASE1, HBA-A1, HMOX1, IFI27L2A, KLF15, LCN2, MT1, PIM3, PIP, S100A8, S100A9, SERPINA3N, SERPINH1 and SPARC.

2.4.2. Screening of potential hub targets. The Pearson correlation coefficient was further performed to analyze the top

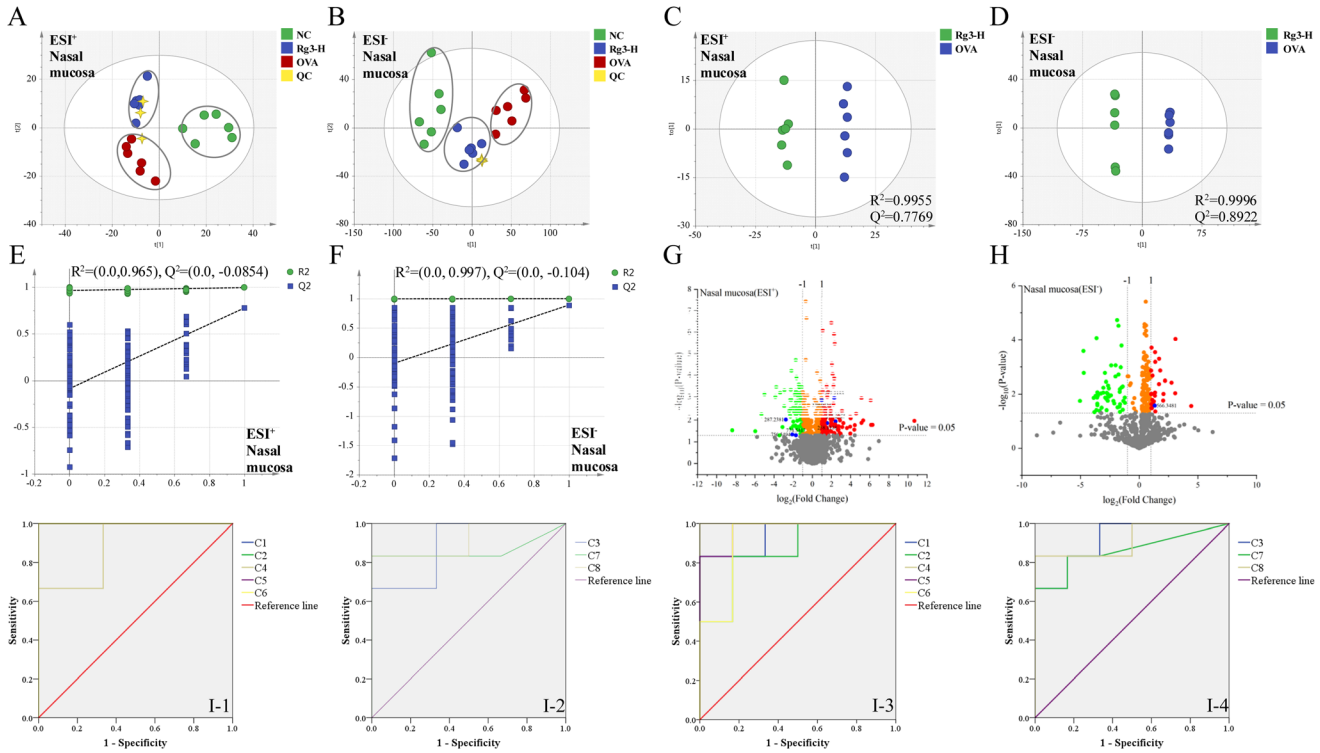

Fig. 3 Metabolomic altered with Rg3 treatment in AR mice. PCA score plots involved ESI^+ (A) and ESI^- (B) of the nasal mucosa samples (n = 6) in NC, OVA and Rg3-H groups. The OPLS-DA score plots involved ESI^+ (C) and ESI^- (D) of the OVA and Rg3-H groups (n = 6). The permutation plots involved ESI^+ (E) and ESI^- (F) of nasal mucosa samples (n = 6) of OVA and Rg3-H groups. The volcanic plots involved ESI^+ (G) and ESI^- (H) of nasal mucosa samples (n = 6) of OVA and Rg3-H groups. (I) The predictive ROC curves generated using 8 biomarkers contributing to AR with Rg3 treatment. (I-1) $C_{OVA} < C_{NC}$; (I-2) $C_{OVA} > C_{NC}$; (I-3) $C_{OVA} < C_{Rg3\text{-}H}$; (I-4) $C_{OVA} > C_{Rg3\text{-}H}$.

Table 1 Distinct metabolites identified in the nasal mucosa samples

No.	t_R/ min	Measured mass (Da)	VIP value	Formula	Mass error (ppm)	Adducts	Biomarkers	HMDB ID	Pathway	Content level
1[b]	0.91	258.1118	1.04	$C_8H_{20}NO_6P$	−6.59	$M + H^+$	Glycerophosphocholine	0000086	Gly M	OVA > Rg3-H ≈ NC
2[b]	0.92	330.0731	1.31	$C_{10}H_{17}N_3O_6S$	−0.23	$M + Na^+$	Glutathione	0062697	Glu M	OVA < Rg3-H ≈ NC
3[b]	18.06	277.2153	1.57	$C_{18}H_{28}O_2$	3.27	$M + H^+$	Stearidonic acid	0006547	α-L M	OVA < Rg3-H ≈ NC
4[b]	18.34	279.2329	1.19	$C_{18}H_{30}O_2$	−3.74	$M + H^+$	α-Linolenic acid	0001388	α-L M	OVA < Rg3-H ≈ NC
5[a]	19.62	566.3481	4.26	$C_{26}H_{52}NO_7P$	−3.11	$M + FA - H^+$	LysoPC(18:1(9Z)/0:0)	0002815	Gly M	OVA > Rg3-H ≈ NC
6[b]	22.65	287.2381	1.01	$C_{20}H_{30}O$	−4.03	$M + H^+$	β-Retinol	0006216	R M	OVA < Rg3-H ≈ NC
7[b]	22.81	756.5494	1.93	$C_{40}H_{80}NO_8P$	2.61	$M + Na^+$	PC(16:0/16:0)	0000564	α-L M Gly M L M	OVA > Rg3-H ≈ NC
8[a]	24.54	774.5417	1.31	$C_{43}H_{78}NO_7P$	−1.15	$M + Na^+$	PE(P-18:0/20:4 (5Z,8Z,11Z,14Z))	0005779	Gly M	OVA > Rg3-H ≈ NC

"Rg3-H" represents the drug intervention group (Rg3-H group); "OVA" represents the AR model group; "NC" represents the normal control group; "<" indicates that the content level of the potential biomarker was significantly lower than that of the other group; ">" indicates that the content level was significantly higher than that of the other group; "≈" indicates that the content level was regulated tending to the normal level. Glycerophospholipid metabolism (Gly M); glutathione metabolism (Glu M); linoleic acid metabolism (L M); α-linolenic acid metabolism (α-L M); retinol metabolism (R M). [a] Metabolites validated by MS data. [b] Metabolites confirmed with standards.

20 DEGs and 8 metabolites and was visualized through the heatmap (Fig. 4B). The horizontal and vertical axes represent metabolites and genes, respectively. The squares corresponding to genes and metabolites tended to be dark red or dark blue, indicating a stronger correlation between genes and metabolites. The range −1 to 1 was used to express the depth of the color. Based on the rule of gene-metabolite interaction with coefficient >0.6 and p value <0.05, a total of 15 genes (CDKN1A, COL1A1, COL1A2, COL3A1, CSN3, CYP26B1, DNASE1, HMOX1, KLF15, LCN2, PIM3, PIP, S100A8, SERPINH1 and SPARC) and all metabolites were screened as potential hub targets.

Table 2 Identification results of potential biomarkers in nasal mucosa

	OVA & NC		OVA & Rg3-H	
Compound no.	AUC	*p*	AUC	*p*
1	1.000	0.004	0.944	0.010
2	1.000	0.004	0.861	0.037
3	0.889	0.025	0.917	0.016
4	0.889	0.025	1.000	0.004
5	1.000	0.004	0.972	0.006
6	1.000	0.004	0.917	0.016
7	0.861	0.037	0.861	0.037
8	0.917	0.016	0.917	0.016

The AUCs and *p* values of the biomarkers in different predictive ROC curves. The numbers were consistent with the no. in Table 1.

2.4.3. Verification of potential hub genes by qRT-PCR. The expression of 15 potential hub genes was validated by using qRT-PCR. A total of 12 genes w lopment of the ere found to have obvious changes in expression. Namely, compared with the OVA group, the levels of COL1A1, COL1A2 and COL3A1 in the Rg3-H group were significantly decreased. In contrast, the levels of CSN3, CYP26B1, DNASE1, HMOX1, KLF15, LCN2, PIM3, PIP and S100A8 in the Rg3-H group were obviously increased (Fig. 5). The above gene expression trends were consistent with the results of previous transcriptome sequencing.

2.4.4. Network construction. The gene-metabolite network (Fig. 6A) was constructed by using the above 12 hub genes and 8 metabolites. Each gray line represents the strong correlation between the genes and the metabolites. For each gene or metabolite, more connecting lines indicated that it might have a stronger impact on the regulatory network. Overall, 12 genes and 8 metabolites were closely correlated.

2.4.5. Pathway enrichment. Aiming at discussing the mechanism of Rg3, the pathways closely related to Rg3 treatment of AR were explored based on these 12 hub genes and 8 metabolites. A total of 4 main pathways including retinol metabolism, glycerophospholipid metabolism, ECM-receptor interaction and α-linolenic acid metabolism were screened out by Jiont-Pathway Analysis (Table 3). Impact values were the result of topological analysis. A higher value indicated a greater topological impact on the pathway. In addition, the bubble map (Fig. 6B) with a descending order of impact value was generated using MetaboAnalyst 5.0. The $-\log10(p)$ values were calculated to demonstrate the difference in the pathway. The size of the circle had a positive correlation with the above 2 parameters. The above 4 pathways have been reported to be related to the occurrence and development of allergic lower airway disease. The retinol metabolism in patients,[33] the glycerophospholipid metabolism in the pathogenesis of disease,[34] ECM-receptor interactions in the regulation of disease,[35] and candidate drug α-linolenic acid for preventing IgE-mediated allergic diseases were studied.[36] Our research results were consistent with the literature.

The network including the hub genes, metabolites and pathways was finally established, as shown in Fig. 6C. The hub genes and metabolites were marked with circles and squares, respectively. Red and blue represented upregulation and downregulation, respectively. Other genes and metabolites are marked in gray.

3. Discussion

It had been reported that ginsenoside Rg3 could diminish allergic lower airway inflammation and oxidative stress.[4] Aiming at exploring the role of Rg3 in allergic upper airway disease, the effect and mechanism of Rg3 on OVA-induced AR (a typical kind of allergic upper airway disease) were revealed in the present study. The results indicated that Rg3 could ameliorate inflammation, oxidative stress and nasal symptoms in

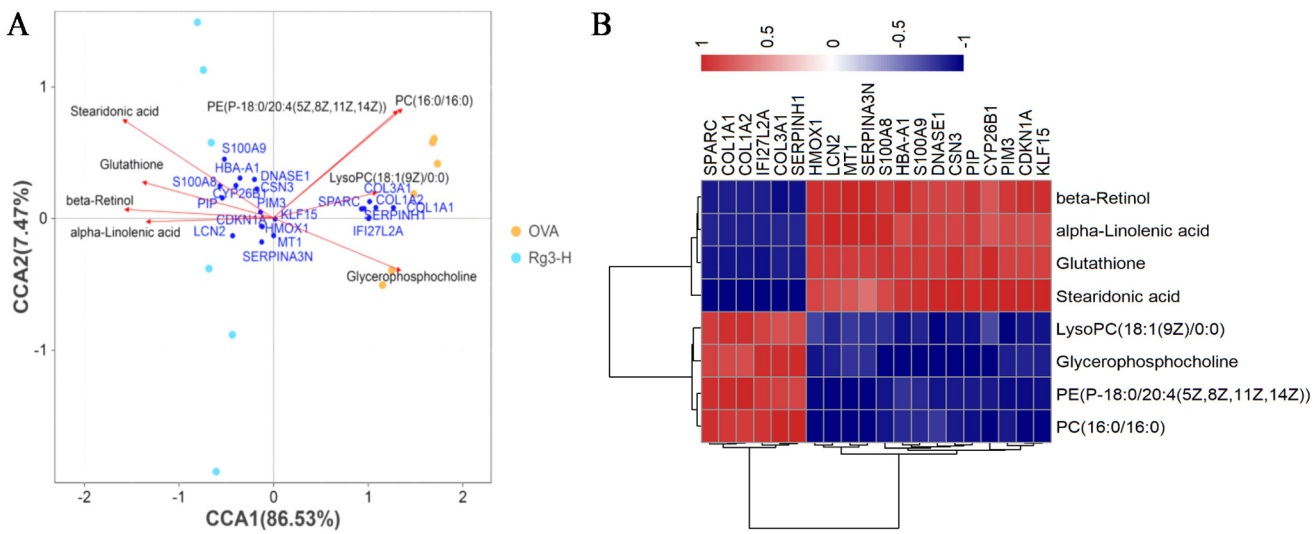

Fig. 4 (A) CCA of top 20 DEGs and 8 differential metabolites in AR mice treated with Rg3. (B) Pearson correlation coefficient of top 20 DEGs and 8 differential metabolites.

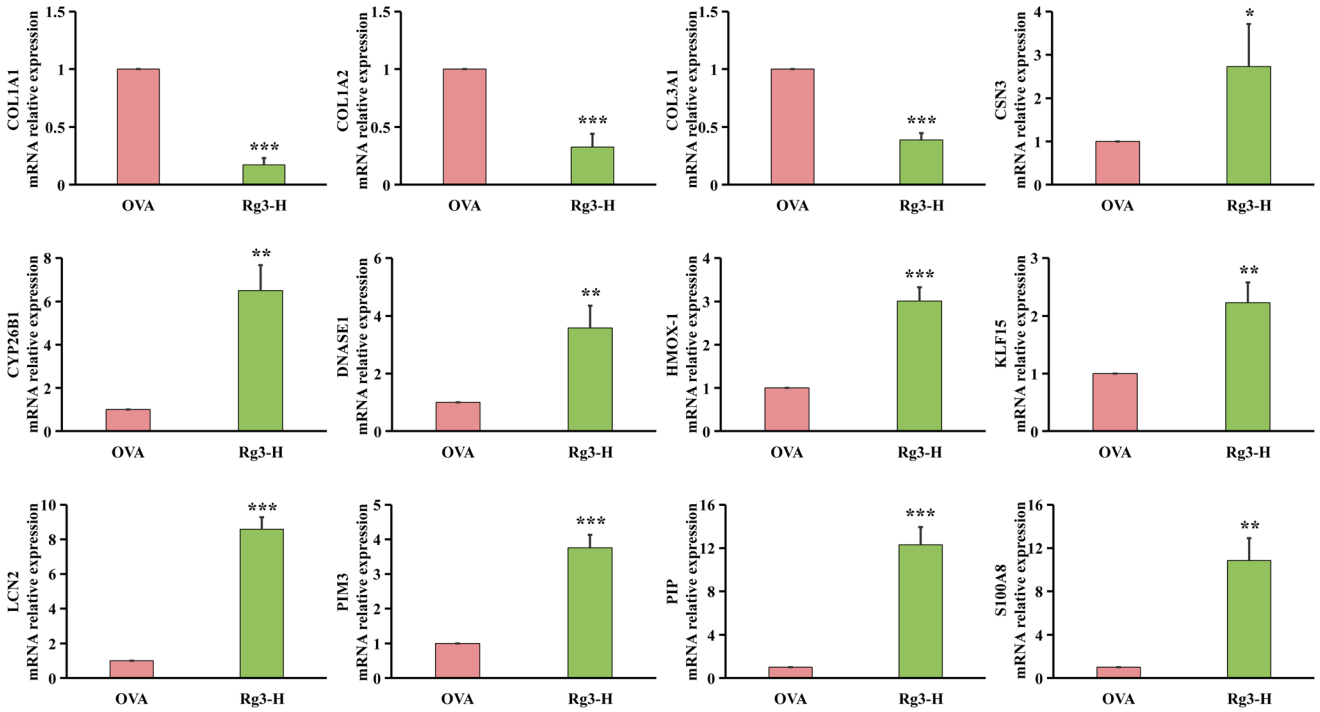

Fig. 5 qRT-PCR results of the OVA group and Rg3-H group (n = 3). Data are presented as mean ± SD. * $p < 0.05$, ** $p < 0.01$, *** $p < 0.001$.

AR mice and might be used as a potential natural agent to influence the course of AR development.

When establishing the animal models, according to the reference, allergic airway inflammation was more obvious in female mice than in male mice after OVA challenge, so female mice were chosen as experiment animals in our study.[37]

Among the 3 downregulated hub genes, COL1A1 was also reported to be closely related to allergic lower airway disease. For example, COL1A1 with high expression appeared in airway smooth muscle cells of allergic lower airway disease.[38,39] For COL1A2, although there were no direct reports to prove its relation to the allergic airway disease, it was inferred that COL1A1 and COL1A2 might have a relationship with each other.[40,41] Regarding another downregulated hub gene, COL3A1, significantly high expression was reported in OVA-induced severe asthma mice.[42] Interestingly, in house dust mite (HDM)-induced allergic lower airway disease, high levels of COL1A1 and COL3A1 were also considered as the important features.[43]

Among the 9 upregulated hub genes, high level of DNASE1 was reported to play an important role in protecting damaged areas by reducing oxidative stress and increasing neutrophil extracellular trap (NET) disintegration.[44–46] Therefore, it could be inferred that high expression of DNASE1 in the Rg3-H group might have a key effect on diminishing allergic lower airway oxidative stress. Another gene, HMOX1, the variation of which might be associated with asthma,[47] had a close relationship with attenuating oxidative stress.[48] For KLF15, it has also been reported that asthma might be aggravated when this gene was suppressed.[49] LCN2 hub gene expression was discovered to be decreased in nasal secretions in asthma patients.[50] In contrast, the elevated level of LCN2 was decreased in patients with improved asthma symptoms.[51] In the literature, we also found that the increased expression of PIM3 played a role in relieving inflammation.[52] In addition, in patients with chronic rhinosinusitis with nasal polyps (CRSwNP) and asthma comorbidity, the level of PIP was found to be decreased.[53] In our study, the level of PIP was significantly increased by the treatment with Rg3. A similar situation occurred in S100A8: namely, in the nasal mucus of AR patients, S100A8 showed a lower level.[54] S100A8 was upregulated by Rg3 in our study. CSN3, a source of bioactive peptides, was produced by *Lactobacillus helveticus*.[55] *Lactobacillus helveticus* could ameliorate the symptoms of perennial AR patients by inhibiting eosinophils in the blood and nasal fluids.[56] Combined with our results, an interesting regulatory pathway was inferred in which Rg3 might influence the modification of microbiomics to mitigate AR inflammation, such as enhancing the ability of *Lactobacillus helveticus* to generate high levels of CSN3. This will be studied in our future work. Finally, although there was no report on the direct association between CYP26B1 and AR, CYP26B1 and β-retinol, were both products of retinol metabolism.

Our research also found a total of 8 metabolites that potentially contribute to AR progression and Rg3 treatment. Among these metabolites, (i) a high level of glycerophosphocholine had been reported to be related to the risk of childhood asthma.[57] (ii) The increase in glutathione could prevent lung airway epithelial cells from enduring oxidant injury in asthma.[58] Additionally, glutathione could ameliorate the

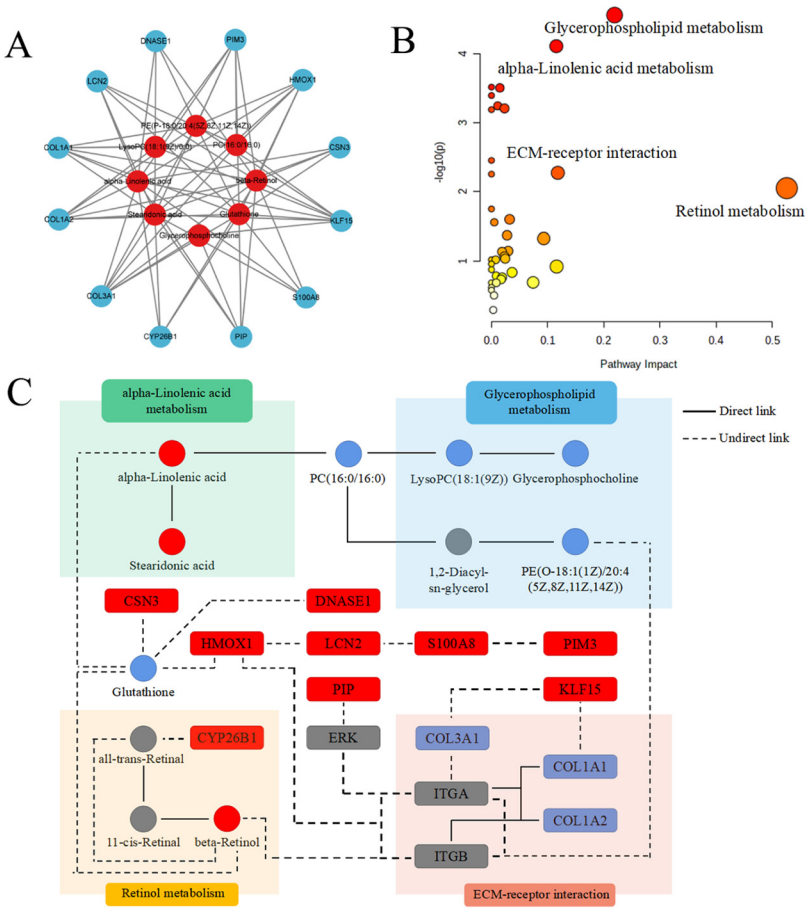

Fig. 6 (A) Gene-metabolite network of hub DEGs and metabolites. (B) The bubble chart of pathways. (C) The interaction network based on transcriptomics and metabolomics.

Table 3 The results from pathways of hub DEGs and metabolites

Pathway name	Match status	p	$-\log10(p)$	Holm p	FDR	Impact
Retinol metabolism	2/116	0.0089	2.0523	1	0.2416	0.5254
Glycerophospholipid metabolism	4/149	2.74×10^{-5}	4.5620	0.0089	0.0089	0.2190
ECM-receptor interaction	2/89	0.0053	2.2752	1	0.1647	0.1181
α-Linolenic acid metabolism	3/69	7.75×10^{-5}	4.1106	0.0253	0.0127	0.1154

imbalance of Treg/Th17 cells by inhibiting intracellular autophagy to be beneficial for the therapy of AR patients.[59] Interestingly, glutathione and HMOX1 might be related to the ferroptosis pathway in AR mice with Rg3 treatment in our study.[60] (iii) Stearidonic acid, a specific combined-long-chain polyunsaturated fatty acid, inhibited of inflammatory process in asthmatic mice.[61] (iv) α-Linolenic acid also showed a similar regulatory trend on OVA-induced bronchoalveolar inflammation in mice.[62] (v) It was reported that the high expression of lysoPC(18:1(9*Z*)/0:0) was present in the airways of allergic patients challenged with antigen.[63] A similar trend was also shown in the OVA group in our study, but was then reregulated by Rg3 treatment. (vi) β-Retinol also had a positive effect on allergic airway inflammatory reactions.[64] Additionally, this metabolite played a crucial role in regulating the immunopathologic mechanisms of asthma by suppressing Th2-type cytokines, hypersecretion of mucus, hyperplasia of goblet cells and histamine levels.[65] (vii) A high level of PC(16:0/16:0) was clearly related to sputum eosinophil cationic protein levels and pulmonary function in the induced sputum of asthmatic children.[66] (viii) PE(P-18:0/20:4(5*Z*,8*Z*,11*Z*,14*Z*)) was one of the main sources of PC(16:0/16:0) in glycerophospholipid metabolism. Therefore, we inferred that it might be indirectly related to the occurrence or development of AR, although there was no report about the direct connection.

Some relevance between mRNA and metabolite based on transcriptomic and metabolomic results could be correlated. For examples: (i) oxidative stress had played an important role in aggravating allergic rhinitis.[67] The increase of HMOX1 and glutathione could alleviate oxidative stress by Nf-E2 related

factor 2 (Nrf2).[68,69] In our analysis of multi-omics study, it was obviously found that Rg3 could upregulate the expressions of HMOX1 and glutathione and had a positive effect on allergic rhinitis. (ii) It is also worth noting that β-retinol had negative association with AR patients.[70] And it was interesting to find that the high level of β-retinol could improve oxidative stress by upregulating the expressions of Nrf2, HMOX1 and glutathione and downregulate the expression of MDA.[71,72] The higher level of β-retinol in the Rg3-H group than in the OVA group was also found in our study. (iii) α-Linolenic acid had a positive effect on diminishing airway inflammation by reversing low levels of glutathione and SOD and high level of MDA.[73] Moreover, the levels of Nrf2 and HMOX1 could also be increased by α-linolenic acid.[74] Our study showed that the level of α-linolenic acid in the Rg3-H group was higher than that in the OVA group. (iv) A high level of S100A8 could play a protective role in allergic inflammation by reducing the production of IL-5 and IL-13 and diminishing eosinophil infiltration.[75]

4. Experimental

4.1. Materials and reagents

Ginsenoside Rg3 (CAS Registry Number: 14197-60-5) with a purity of above 99% was provided by the Natural Product Research Center of Jilin University.

Glycerophosphocholine was purchased from Shanghai Zhen Zhun Biological Technology Co., Ltd (China). α-Linolenic acid was purchased from the National Institutes for Food and Drug Control (China). Stearidonic acid and PC(16:0/16:0) were purchased from Merck (Germany). β-Retinol was provided by Shanghai Aladdin Biochemical Co., Ltd (China). Glutathione, OVA, and DEX were all purchased from Sigma-Aldrich (USA).

LC-MS grade acetonitrile and methanol were purchased from Fisher Chemical Company (Belgium). Purified water was purchased from A.S. Watson Group Ltd (China).

A mouse IgE ELISA kit was purchased from Abcam company (USA). Mouse IL-4, IL-5, and IL-13 ELISA kits were purchased from Raybiotech (USA). ELISA kits for MDA and SOD were purchased from Shanghai Biyuntian Biotechnology Co., Ltd (China). Agcourt AMPure XP beads were provided by Beckman Coulter Inc. (USA). A Thermo Scientific kit was purchased from Thermo Fisher Scientific (USA). TRIzol reagent for RNA-sequencing was provided by Life Technologies (USA).

The inhalation tower, controller system and Buxco pulmonary function testing system were purchased from Data Sciences International (USA). A Waters Xevo G2-XS QTOF mass spectrometer (USA) and a Waters ultraperformance liquid chromatography (USA)system were used. An Agilent 2100 Bioanalyzer was provided by Agilent Technologies (USA). The Bio-Rad Minioption RT-PCR detection system was provided by Bio-Rad (Hercules, USA).

4.2. Animals and administration

Female specific pathogen-free (SPF) BALB/c mice (18 g–22 g) were purchased from Changchun Yisi Experimental Animal Technology Co., Ltd (China). They were housed in a cabinet maintained at 21–23 °C at a relative humidity of 40%–60% with a 12 h dark/light cycle throughout the study.

Animal experiments were performed in accordance with the guidelines for the care and use of laboratory animals (protocol no. 2021-401) and were approved by Institutional Animal Care and Use Committee of Jilin University.

After one week of acclimatization, the mice were randomly divided into 6 groups: NC group, OVA-induced model group (OVA group), OVA-induced + DEX group (2.0 mg kg^{-1} day^{-1}, DEX group), and OVA-induced + Rg3 groups (5, 10, 20 mg kg^{-1} day^{-1}, Rg3-L, M, H groups). For animal treatment, Rg3 (0.5, 1.0, 2.0 mg ml^{-1}) and DEX (0.2 mg ml^{-1}) were suspended in water and were intragastrically administered to mice at 10 ml kg^{-1}.

Except for the NC group, all the mice in the other groups were sensitized by an intraperitoneal injection of 100 μg of OVA and 2 mg of aluminum hydroxide (mixed in 200 μl of normal sterile saline) on days 0, 7, and 14. They were subsequently challenged with 5% OVA by using the nose-only exposure system (Buxco Inhalation Tower All-In-One Controller) from day 21 to day 27. The NC group mice were sham-sensitized and challenged with an equivalent volume of normal saline at the same time. On days 21–27, intragastric administration of Rg3 or dexamethasone was carried out. Every drug intervention was administered 2 hours prior to OVA challenge. The NC group and OVA group were given equal amounts of saline. The schematic design for establishing the mouse model and administration is shown in Fig. 7.

4.3. Evaluation of the effect of Rg3 on AR

On day 28, the number of nose rubbing and sneezing events over a duration of 10 min after the final OVA nasal challenge was recorded. Whole blood samples were collected from the orbit and centrifuged at 4000 rpm for 10 min to obtain the serum supernatants. The levels of IgE, IL-4, IL-5, IL-13, MDA and SOD in serum were measured by using commercial ELISA kits following the manufacturer's instructions. The nasal tissues were collected and the nasal mucosa from nasal tissues located in the nasal septum and nasal cavity was slowly separated and gently washed in saline. Some nasal mucosa samples were fixed in 4% paraformaldehyde, paraffinized, cut into sections, and finally stained with H&E (hematoxylin and eosin)

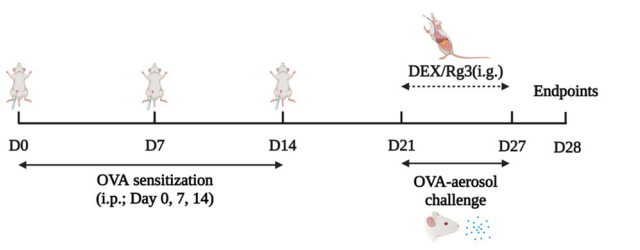

Fig. 7 The experimental process of the AR model establishment and administration.

for histopathological examination. Other nasal mucosa samples were stored at −80 °C for transcriptomic and metabolomic studies.

4.4. Transcriptomics analysis

The nasal mucosa samples of the NC, OVA and Rg3-H groups (n = 6) were used to perform the transcriptomic analysis.

4.4.1. RNA extraction, library construction, and RNA sequencing. Total RNA was extracted from nasal mucosa according to the TRIzol reagent instructions. The integrity and concentration of RNA were detected, and the mRNA was separated following the manufacturer's instructions. Briefly, the enriched mRNA was split into approximately 200 nt RNA inserts for the synthesis of first-strand cDNA and second-strand cDNA. The double-stranded cDNA was subjected to end-repair/dA-tail and adaptor ligation. Then, suitable fragments were obtained for isolation and enriched by polymerase chain reaction (PCR) amplification. Finally, the established libraries of experimental mice were analyzed using the Illumina HiSeq™ sequencing platform. All the above processes were completed by Biomarker Technologies (Beijing, China).

4.4.2. Principal component analysis. PCA of gene expression profiles obtained by RNA sequencing of three groups of the nasal mucosa was performed by using the platform BMKCloud (**https://www.biocloud.net**).

4.4.3. Analysis of DEGs. The DEseq2 algorithm based on the platform BMKCloud (**https://www.biocloud.net**) was used to screen DEGs between the NC group, OVA group and Rg3-H group.[76,77] The fold change threshold was set at $|\log_2\text{fold change}| \geq 1$ and the adjusted p value was set as <0.05. A Venn diagram was then used to screen the key DEGs that contributed to the effect of Rg3. Only the DEGs that tended to the level expressed in the NC group could be considered as the key DEGs that played an important role in the treatment of AR with Rg3. The levels of DEGs were visualized through a heatmap based on the R package pheatmap.[78]

4.5. Metabolomics analysis

The nasal mucosa samples of the NC, OVA and Rg3-H groups (n = 6) were used to analyze the metabolic profiles using the UPLC-Q/TOF-MS method in both positive and negative modes.

4.5.1. Preparation of test samples. After being thawed at room temperature, an appropriate amount of nasal mucosa, homogenized with 2-fold volume of saline, was added to 10-fold volume of methanol and then vortexed for 3 min. After that, the mixture was centrifuged at 10 000 rpm for 10 min at 4 °C. The supernatant obtained was dried in a gentle stream of nitrogen at 37 °C. Finally, the residue was redissolved in 100 μl of 80% methanol and filtered through a 0.22 μm filter, and the test samples were obtained. Meanwhile, a 10 μl aliquot of each test sample group was mixed to prepare a quality control (QC) sample.

4.5.2. UPLC-Q/TOF-MS conditions

LC conditions. Chromatographic separation was performed on an ACQUITY UPLC BEH C18 column (100 mm × 2.1 mm, 1.7 μm, Waters Co.) at a temperature of 30 °C. The temperature of the sample manager was set at 4 °C. The mobile phases were composed of 0.1% formic acid in water (A) and 0.1% formic acid in acetonitrile (B), at a flow rate of 0.4 ml min^{-1}. The elution requirement was as follows: 0–2 min, 10% B; 2–26 min, 10→90% B; 26–28 min, 90% B; 28–28.1 min, 90→10% B. Then, 90% and 10% acetonitrile were used as the strong wash solvent and weak wash solvent, respectively.

MS conditions. MS analysis was performed with an electrospray ionization (ESI) interface in the positive or negative mode. The mass spectrum was collected in the MS^E centroid mode with a low energy of 6 V and a high energy of 20–40 V. The optimized MS parameters applied were as follows: cone gas flow rate of 60 L h^{-1}, cone voltage of 38 V, source temperature of 150 °C, desolvation temperature of 360 °C, desolvation gas flow of 1000 L h^{-1}, capillary voltage in the positive ion mode at 2.9 kV and in the negative ion mode at 3.0 kV. Leucine enkephalin (200 ng ml^{-1}, m/z 556.2771 in the ESI^+ mode and m/z 554.2615 in the ESI^- mode) with a constant flow at 10 μl min^{-1} as an external reference of Lock Spray™. The QC sample was injected randomly 5 times throughout the entire worklist. The injection volume for all samples was 5 μl for each run. Leucine enkephalin with a constant flow at 10 μl min^{-1} was used as an external reference of Lock Spray™. To ensure mass reproducibility and accuracy, the mass spectrometer was calibrated with sodium formate within the range of 50–1200 Da. Data recording was carried out on a MassLynx V4.1 workstation (Waters, Manchester, UK).

4.5.3. Validation of UPLC-QTOF-MS. The assay method should be validated, including system stability, precision, reproducibility and sample stability. The detailed methods are as follows: the mass/RT (min) pairs of different mass ions in randomly run QC samples were used to monitor system stability; precision was estimated by consecutively detecting five QC replicates; reproducibility was assessed by analyzing five replicates of one serum sample; and one serum test sample placed in an autosampler for 0, 8, 12, and 16 h at 4 °C was monitored to evaluate the stability of the sample. The RSDs of peak intensity and RT should be calculated in all of the above investigations.

4.5.4. Metabolomics analysis. MarkerLynx XS V4.1 software (Waters, Milford, CT, USA) was used to perform calibration, deconvolution, data reduction, chromatographic peak extraction and normalization of the data. The identical components in various samples should have similar values of RT and m/z. The major processing parameters were set as follows: mass tolerance of 0.10, retention time window of 0.10, a minimum intensity of 15%, marker intensity threshold of 3000 counts, and noise elimination level 7. The resulting data were then multivariate statistically analyzed. PCA, OPLS-DA and permutation tests were all performed. The differential metabolites were explored by variable importance for the projection (VIP) and volcano plots. Metabolites with VIP > 1.0 and p < 0.05 were considered potential metabolic biomarkers. Furthermore, predictive ROC curves were generated to assess the above results. The better result was that the area under the ROC curve should be more than 0.8. The potential biomarkers

screened above were further identified by comparison with reference standards, accurate molecular weights or fragmentation patterns based on HMDB (https://www.hmdb.ca/), METLIN databases (https://metlin.scripps.edu/), KEGG (https://www.kegg.com/) and Metabo-Analyst (https://www.metaboanalyst.ca/). The mass tolerance should be within ±10 ppm.

4.6. Integrated analysis involving transcriptomics and metabolomics

The correlation analysis of expressed genes and metabolite accumulation was carried out based on the transcriptomics and metabolomics data. The information about metabolites with differential accumulation could assist in the "coexpression" analysis of genes. As a result, the core regulatory network was built, and functional hub genes were found.

4.6.1. Canonical correlation analysis. CCA was performed to mine the correlation between sets of variables of multiomics data.[32] The correlation of DEGs and differential metabolites was measured by using CCA. The content levels of differential metabolites and the expression levels of DEGs were imported into software Canoco 5.0 (https://www.canoco5.com/) and the OmicShare database (https://omicshare.com/) with default parameters for CCA.[79]

4.6.2. Expression analysis of potential hub genes by qRT-PCR. DEGs and differential metabolites from CCA were analyzed by the Pearson correlation coefficient.[32] Only the gene–metabolite interaction with Pearson correlation coefficient >0.6 and p value <0.05 was chosen to be significant,[80,81] and the genes and metabolites were considered as the potential hub genes and metabolites. The expression of potential hub genes was then analyzed by qRT-PCR as follows: total RNA was obtained from the mouse nasal mucosa by using TRIzol reagent. Complementary DNA (cDNA) was extracted by using a Thermo Scientific kit according to the manufacturer's instructions. qRT-PCR analysis was performed after 40 cycles by using a Bio-Rad Minioption RT-PCR detection system and SYBR Green Super Mix. The sequences of the primers used in qRT-PCR are shown in Table S1.† The gene expression of β-actin and DEGs identified by CCA and Pearson correlation coefficient was calculated by the $2^{-\Delta\Delta Ct}$ method.

4.6.3. Network construction. The PCR validated genes and differential metabolites that were considered as hub genes and metabolites were imported into Cytoscape software to create the gene-metabolite network.[82]

4.6.4. Joint-pathway analysis. The hub genes and metabolites from the network were analyzed by Joint-Pathway Analysis (https://www.metaboanalyst.ca/) based on KEGG (https://www.kegg.com/).[83] The main pathways affected by Rg3 acting on AR were mined according to the impact values of pathways enriched by Joint-Pathway Analysis.

4.7. Statistical analysis

All analyses were performed using GraphPad Prism version 6.0 software (CA, USA). The results are presented as the mean ± SD. Comparisons between groups were conducted with a two-tailed test or one-way analysis of variance (ANOVA). Data significance was accepted when $p < 0.05$.

5. Conclusion

Allergic rhinitis, a kind of allergic upper airway disease, is a common global public health problem. In the present study, nasal symptoms, biochemical parameters in serum and histopathological examination of nasal mucosa were used to evaluate the effects of Rg3 on OVA-induced AR model mice for the first time. Transcriptomics and metabolomics were used to explore the therapeutic mechanism. After intragastric administration of Rg3, the nasal symptoms were effectively improved, and the levels of IgE, IL-4, IL-5, IL-13 and MDA in serum were significantly reduced, while the levels of SOD were obviously increased. Moreover, the inflammatory cell infiltration in the Rg3 group mice was significantly reduced. The anti-AR effect of Rg3 was closely associated with the regulation of 12 DEGs and 8 differential metabolites. In addition, these targets might be involved in 4 main pathways. In summary, Rg3 has a therapeutic effect on OVA-induced AR in mice by inhibiting inflammation development and reducing oxidative stress. The mechanism was related to the gene-metabolite interaction network. This study could provide a potential natural agent for the treatment of AR and is beneficial for mining and expanding the worth of Rg3.

Author contributions

The authors confirm the contribution to the paper as follows: conceptualization, Jianming Liu; methodology, Jianming Liu, Fang Wang and Dongdong Zhu; software, Xingcheng Yi and Cuizhu Wang; validation, Jianming Liu, Guoqiang Wang and Na Yang; formal analysis, Jianming Liu and Hongqiang Lin; investigation, Jianming Liu, Cuizhu Wang, Liwei Sun, and Guoqiang Wang; data curation, Jianming Liu, Xingcheng Yi and Na Yang; writing—original draft preparation, Jianming Liu; writing—review and editing, Fang Wang and Dongdong Zhu; supervision, Fang Wang and Dongdong Zhu; funding acquisition, Dongdong Zhu. All authors had performed comprehensive review of the results and confirmed the last version of the manuscript.

Conflicts of interest

There are no conflicts to declare.

Acknowledgements

This research was funded by the National Natural Science Foundation of China (81870701, 82071016), the Natural Science Foundation of Jilin Province (20200201600JC, 20200201200JC, 20200201411JC), the Jilin Province Health

Science and Technology Talent Project (2021SCZ42, 2020SCZ24), the Innovation Capacity Construction Project of Jilin Province (2021C009) and the China–Japan Union Hospital of Jilin University-College of Basic Medical Sciences of Jilin University Project (KYXZ2022JC08).

References

1 T. Chen, L. Xiao, L. Zhu, S. Ma, T. Yan and H. Ji, Anti-Asthmatic Effects of Ginsenoside Rb1 in a Mouse Model of Allergic Asthma Through Relegating Th1/Th2, *Inflammation*, 2015, **38**(5), 1814–1822, DOI: **10.1007/s10753-015-0159-4**. PMID: 25832478.

2 H. I. Kim, J. K. Kim, J. Y. Kim, M. J. Han and D. H. Kim, Fermented red ginseng and ginsenoside Rd alleviate ovalbumin-induced allergic rhinitis in mice by suppressing IgE, interleukin-4, and interleukin-5 expression, *J. Ginseng Res.*, 2019, **43**(4), 635–644, DOI: **10.1016/j.jgr.2019.02.006**. Epub 2019 Mar 7. PMID: 31695569; PMCID: PMC6823749.

3 H. A. Oh, J. Y. Seo, H. J. Jeong and H. M. Kim, Ginsenoside Rg1 inhibits the TSLP production in allergic rhinitis mice, *Immunopharmacol. Immunotoxicol.*, 2013, **35**(6), 678–686, DOI: **10.3109/08923973.2013.837061**. Epub 2013 Sep 20. PMID: 24053327.

4 W. C. Huang, T. H. Huang, K. W. Yeh, Y. L. Chen, S. C. Shen and C. J. Liou, Ginsenoside Rg3 ameliorates allergic airway inflammation and oxidative stress in mice, *J. Ginseng Res.*, 2021, **45**(6), 654–664, DOI: **10.1016/j.jgr.2021.03.002**. Epub 2021 Mar 13. PMID: 34764720; PMCID: PMC8569325.

5 Q. Li, C. Zhai, G. Wang, J. Zhou, W. Li, L. Xie, *et al.*, Ginsenoside Rh1 attenuates ovalbumin-induced asthma by regulating Th1/Th2 cytokines balance, *Biosci., Biotechnol., Biochem.*, 2021, **85**(8), 1809–1817, DOI: **10.1093/bbb/zbab099**.

6 L. C. Li, H. M. Piao, M. Y. Zheng, Z. H. Lin, Y. H. Choi and G. H. Yan, Ginsenoside Rh2 attenuates allergic airway inflammation by modulating nuclear factor-κB activation in a murine model of asthma, *Mol. Med. Rep.*, 2015, **12**(5), 6946–6954, DOI: **10.3892/mmr.2015.4272**. PMID: 26502836.

7 C. Y. Lim, J. M. Moon, B. Y. Kim, S. H. Lim, G. S. Lee, H. S. Yu, *et al.*, Comparative study of Korean White Ginseng and Korean Red Ginseng on efficacies of OVA-induced asthma model in mice, *J. Ginseng Res.*, 2015, **39**(1), 38–45, DOI: **10.1016/j.jgr.2014.07.004**. Epub 2014 Aug 1. PMID: 25535475; PMCID: PMC4268570.

8 L. W. Qi, C. Z. Wang and C. S. Yuan, Isolation and analysis of ginseng: advances and challenges, *Nat. Prod. Rep.*, 2011, **28**(3), 467–495, DOI: **10.1039/c0np00057d**. Epub 2011 Jan 24. PMID: 21258738; PMCID: PMC3056508.

9 H. I. Kim, J. K. Kim, J. Y. Kim, M. J. Han and D. H. Kim, Fermented red ginseng and ginsenoside Rd alleviate ovalbumin-induced allergic rhinitis in mice by suppressing IgE, interleukin-4, and interleukin-5 expression, *J. Ginseng Res.*, 2019, **43**(4), 635–644, DOI: **10.1016/j.jgr.2019.02.006**. Epub 2019 Mar 7. PMID: 31695569; PMCID: PMC6823749.

10 C. H. Ma, W. C. Chou, C. H. Wu, I. M. Jou, Y. K. Tu, P. L. Hsieh, *et al.*, Ginsenoside Rg3 Attenuates TNF-α-Induced Damage in Chondrocytes through Regulating SIRT1-Mediated Anti-Apoptotic and Anti-Inflammatory Mechanisms, *Antioxidants*, 2021, **10**(12), 1972, DOI: **10.3390/antiox10121972**. PMID: 34943075; PMCID: PMC8750552.

11 K. Zhang, Y. Liu, C. Wang, J. Li, L. Xiong, Z. Wang, *et al.*, Evaluation of the gastroprotective effects of 20 (S)-ginsenoside Rg3 on gastric ulcer models in mice, *J. Ginseng Res.*, 2019, **43**(4), 550–561, DOI: **10.1016/j.jgr.2018.04.001**. Epub 2018 Apr 9. PMID: 31695563; PMCID: PMC6823781.

12 J. Hou, J. Xue, Z. Wang and W. Li, Ginsenoside Rg3 and Rh2 protect trimethyltin-induced neurotoxicity via prevention on neuronal apoptosis and neuroinflammation, *Phytother. Res.*, 2018, **32**(12), 2531–2540, DOI: **10.1002/ptr.6193**. Epub 2018 Oct 2. PMID: 30277284.

13 W. Tang, Y. Zhang, J. Gao, X. Ding and S. Gao, The anti-fatigue effect of 20(R)-ginsenoside Rg3 in mice by intranasally administration, *Biol. Pharm. Bull.*, 2008, **31**(11), 2024–2027, DOI: **10.1248/bpb.31.2024**. PMID: 18981567.

14 H. Lee, Y. Hong, Q. Tran, H. Cho, M. Kim, C. Kim, *et al.*, A new role for the ginsenoside RG3 in antiaging via mitochondria function in ultraviolet-irradiated human dermal fibroblasts, *J. Ginseng Res.*, 2019, **43**(3), 431–441, DOI: **10.1016/j.jgr.2018.07.003**. Epub 2018 Jul 31. PMID: 31308815; PMCID: PMC6606973.

15 Y. Zhang, S. Wang, S. Song, X. Yang and G. Jin, Ginsenoside Rg3 Alleviates Complete Freund's Adjuvant-Induced Rheumatoid Arthritis in Mice by Regulating CD4+CD25+Foxp3+Treg Cells, *J. Agric. Food Chem.*, 2020, **68**(17), 4893–4902, DOI: **10.1021/acs.jafc.0c01473**. Epub 2020 Apr 21. PMID: 32275817.

16 I. S. Lee, I. Uh, K. S. Kim, K. H. Kim, J. Park, Y. Kim, *et al.*, Anti-Inflammatory Effects of Ginsenoside Rg3 via NF-κB Pathway in A549 Cells and Human Asthmatic Lung Tissue, *J. Immunol. Res.*, 2016, **2016**, 7521601, DOI: **10.1155/2016/7521601**. Epub 2016 Dec 27. PMID: 28116321; PMCID: PMC5223042.

17 J. Y. Kee and S. H. Hong, Ginsenoside Rg3 suppresses mast cell-mediated allergic inflammation via mitogen-activated protein kinase signaling pathway, *J. Ginseng Res.*, 2019, **43**(2), 282–290, DOI: **10.1016/j.jgr.2018.02.008**. Epub 2018 Mar 1. PMID: 30976166; PMCID: PMC6437450.

18 L. Cheng, J. Chen, Q. Fu, S. He, H. Li, Z. Liu, *et al.*, Chinese Society of Allergy Guidelines for Diagnosis and Treatment of Allergic Rhinitis, *Allergy, Asthma Immunol. Res.*, 2018, **10**(4), 300–353, DOI: **10.4168/aair.2018.10.4.300**. PMID: 29949830; PMCID: PMC6021586.

19 J. Bousquet, J. M. Anto, C. Bachert, I. Baiardini, S. Bosnic-Anticevich, G. Walter Canonica, *et al.*, Allergic rhinitis, *Nat. Rev. Dis. Primers*, 2020, **6**(1), 95, DOI: **10.1038/s41572-020-00227-0**. PMID: 33273461.

20 J. L. Brożek, J. Bousquet, I. Agache, A. Agarwal, C. Bachert, S. Bosnic-Anticevich, *et al.*, Allergic Rhinitis and its Impact

on Asthma (ARIA) guidelines-2016 revision, *J. Allergy Clin. Immunol.*, 2017, **140**(4), 950–958, DOI: **10.1016/j.jaci.2017.03.050**. Epub 2017 Jun 8. PMID: 28602936.

21 K. H. I. N. M. Herath, H. J. Kim, S. P. Mihindukulasooriya, A. Kim, H. J. Kim, Y. J. Jeon, *et al.*, Sargassum horneri extract containing mojabanchromanol attenuates the particulate matter exacerbated allergic asthma through reduction of Th2 and Th17 response in mice, *Environ. Pollut.*, 2020, **265**(Pt B), 114094, DOI: **10.1016/j.envpol.2020.114094**. Epub 2020 Feb 20. PMID: 32806433.

22 Y. Y. Kim, I. G. Je, M. J. Kim, B. C. Kang, Y. A. Choi, M. C. Baek, *et al.*, 2-Hydroxy-3-methoxybenzoic acid attenuates mast cell-mediated allergic reaction in mice via modulation of the FcεRI signaling pathway, *Acta Pharmacol. Sin.*, 2017, **38**(1), 90–99, DOI: **10.1038/aps.2016.112**. Epub 2016 Nov 28. Erratum in: *Acta Pharmacol. Sin.*, 2017, **38**(3), 444. PMID: 27890918; PMCID: PMC5220539.

23 T. T. Bui, D. A. Kwon, D. W. Choi, S. Y. Jung, S. Y. Lee, C. H. Piao, *et al.*, Rosae multiflorae fructus extract and its four active components alleviate ovalbumin-induced allergic inflammatory responses via regulation of Th1/Th2 imbalance in BALB/c rhinitis mice, *Phytomedicine*, 2019, **55**, 238–248, DOI: **10.1016/j.phymed.2018.06.044**. Epub 2018 Aug 11. PMID: 30668435.

24 S. H. Yang and C. L. Yu, Antiinflammatory effects of Buzhong-yi-qi-tang in patients with perennial allergic rhinitis, *J. Ethnopharmacol.*, 2008, **115**(1), 104–109, DOI: **10.1016/j.jep.2007.09.011**. Epub 2007 Sep 19. PMID: 17980528.

25 J. H. Jung, T. K. Kang, J. H. Oh, J. U. Jeong, K. P. Ko and S. T. Kim, The Effect of Korean Red Ginseng on Symptoms and Inflammation in Patients With Allergic Rhinitis, *Ear, Nose Throat J.*, 2021, **100**(5_suppl), 712S–719S, DOI: **10.1177/0145561320907172**. Epub 2020 Feb 19. PMID: 32070136.

26 D. Obeso, L. Mera-Berriatua, J. Rodríguez-Coira, D. Rosace, P. Fernández, I. A. Martín-Antoniano, *et al.*, Multi-omics analysis points to altered platelet functions in severe food-associated respiratory allergy, *Allergy*, 2018, **73**(11), 2137–2149, DOI: **10.1111/all.13563**. Epub 2018 Aug 9. PMID: 30028518.

27 S. J. Gadher, M. Marchetti-Deschmann, G. Allmaier and H. Kovarova, Tremendous progress in proteomics and metabolomics in Central and Eastern Europe, *Expert Rev. Proteomics*, 2015, **12**(1), 9–11, DOI: **10.1586/14789450.2015.989987**. Epub 2014 Dec 8. PMID: 25482208.

28 B. R. Leaker, V. A. Malkov, R. Mogg, M. K. Ruddy, G. C. Nicholson, A. J. Tan, *et al.*, The nasal mucosal late allergic reaction to grass pollen involves type 2 inflammation (IL-5 and IL-13), the inflammasome (IL-1β), and complement, *Mucosal Immunol.*, 2017, **10**(2), 408–420, DOI: **10.1038/mi.2016.74**. Epub 2016 Sep 28. PMID: 27677865.

29 S. Xie, H. Zhang, Z. Xie, Y. Liu, K. Gao, J. Zhang, *et al.*, Identification of Novel Biomarkers for Evaluating Disease Severity in House-Dust-Mite-Induced Allergic Rhinitis by Serum Metabolomics, *Dis. Markers*, 2021, **2021**, 5558458, DOI: **10.1155/2021/5558458**. PMID: 34113404; PMCID: PMC8154289.

30 Q. Shou, L. Jin, J. Lang, Q. Shan, Z. Ni, C. Cheng, *et al.*, Integration of Metabolomics and Transcriptomics Reveals the Therapeutic Mechanism Underlying Paeoniflorin for the Treatment of Allergic Asthma, *Front. Pharmacol.*, 2019, **9**, 1531, DOI: **10.3389/fphar.2018.01531**. PMID: 30761008; PMCID: PMC6362974.

31 S. Y. Ma, N. Zhao, L. Cui, Y. Li, H. Zhang, J. Wang, *et al.*, Therapeutic Effects of Human Pluripotent Stem Cell-Derived Mesenchymal Stem Cells on a Murine Model of Acute Type-2-Dominated Airway Inflammation, *Stem Cell Rev. Rep.*, 2022, **18**(8), 2939–2951, DOI: **10.1007/s12015-022-10389-x**. Epub 2022 May 27. PMID: 35622293.

32 H. Wang, Y. Hu, Y. Xie, L. Wang, J. Wang, L. Lei, *et al.*, Prediction of MicroRNA and Gene Target in Synovium-Associated Pain of Knee Osteoarthritis Based on Canonical Correlation Analysis, *BioMed Res. Int.*, 2019, **2019**, 4506876, DOI: **10.1155/2019/4506876**. PMID: 31737663; PMCID: PMC6815580.

33 Z. Pang, G. Wang, C. Wang, W. Zhang, J. Liu and F. Wang, Serum Metabolomics Analysis of Asthma in Different Inflammatory Phenotypes: A Cross-Sectional Study in Northeast China, *BioMed Res. Int.*, 2018, **2018**, 2860521, DOI: **10.1155/2018/2860521**. PMID: 30345296; PMCID: PMC6174811.

34 K. D. Quinn, M. Schedel, Y. Nkrumah-Elie, A. Joetham, M. Armstrong, C. Cruickshank-Quinn, *et al.*, Dysregulation of metabolic pathways in a mouse model of allergic asthma, *Allergy*, 2017, **72**(9), 1327–1337, DOI: **10.1111/all.13144**. Epub 2017 Mar 29. PMID: 28213886.

35 D. Fussbroich, C. Kohnle, T. Schwenger, C. Driessler, R. P. Dücker, O. Eickmeier, *et al.*, A combination of LCPUFAs regulates the expression of miRNA-146a-5p in a murine asthma model and human alveolar cells, *Prostaglandins Other Lipid Mediators*, 2020, **147**, 106378, DOI: **10.1016/j.prostaglandins.2019.106378**. Epub 2019 Nov 4. PMID: 31698144.

36 Y. Wang, Y. Ding, C. Li, J. Gao, X. Wang and H. An, Alpha-linolenic acid inhibits IgE-mediated anaphylaxis by inhibiting Lyn kinase and suppressing mast cell activation, *Int. Immunopharmacol.*, 2022, **103**, 108449, DOI: **10.1016/j.intimp.2021.108449**. Epub 2021 Dec 17. PMID: 34929479.

37 B. N. Melgert, D. S. Postma, I. Kuipers, M. Geerlings, M. A. Luinge, B. W. van der Strate, *et al.*, Female mice are more susceptible to the development of allergic airway inflammation than male mice, *Clin. Exp. Allergy*, 2005, **35**(11), 1496–1503, DOI: **10.1111/j.1365-2222.2005.02362.x**. PMID: 16297148.

38 I. Janulaityte, A. Januskevicius, V. Kalinauskaite-Zukauske, J. Palacionyte and K. Malakauskas, Asthmatic Eosinophils Promote Contractility and Migration of Airway Smooth Muscle Cells and Pulmonary Fibroblasts In Vitro, *Cells*, 2021, **10**(6), 1389, DOI: **10.3390/cells10061389**. PMID: 34199925; PMCID: PMC8229663.

39 I. Janulaityte, A. Januskevicius, V. Kalinauskaite-Zukauske, I. Bajoriuniene and K. Malakauskas, In Vivo Allergen-Activated Eosinophils Promote Collagen I and Fibronectin

Gene Expression in Airway Smooth Muscle Cells via TGF-β1 Signaling Pathway in Asthma, *Int. J. Mol. Sci.*, 2020, **21**(5), 1837, DOI: **10.3390/ijms21051837**. PMID: 32155894; PMCID: PMC7084581.

40 J. Emsley, C. G. Knight, R. W. Farndale, M. J. Barnes and R. C. Liddington, Structural basis of collagen recognition by integrin alpha2beta1, *Cell*, 2000, **101**(1), 47–56, DOI: **10.1016/S0092-8674(00)80622-4**. PMID: 10778855.

41 J. Heino, The collagen family members as cell adhesion proteins, *Bioessays*, 2007, **29**(10), 1001–1010, DOI: **10.1002/bies.20636**. PMID: 17876790.

42 Y. Qian, Y. Sun, Y. Chen, Z. Mao, Y. Shi, D. Wu, *et al.*, Nrf2 regulates downstream genes by targeting miR-29b in severe asthma and the role of grape seed proanthocyanidin extract in a murine model of steroid-insensitive asthma, *Pharm. Biol.*, 2022, **60**(1), 347–358, DOI: **10.1080/13880209.2022.2032205**. PMID: 35171066; PMCID: PMC8856085.

43 X. Yao, C. Dai, K. Fredriksson, P. K. Dagur, J. P. McCoy, X. Qu, *et al.*, 5A, an apolipoprotein A-I mimetic peptide, attenuates the induction of house dust mite-induced asthma, *J. Immunol.*, 2011, **186**(1), 576–583, DOI: **10.4049/jimmunol.1001534**. Epub 2010 Nov 29. PMID: 21115733; PMCID: PMC3012266.

44 M. Boettcher, D. Meier, M. Jiménez-Alcázar, G. Eschenburg, S. Mietzsch, D. Vincent, *et al.*, Degradation of Extracellular DNA by DNase1 Significantly Reduces Testicular Damage After Testicular Torsion in Rats, *Urology*, 2017, **109**, 223.e1–223.e7, DOI: **10.1016/j.urology.2017.07.031**. Epub 2017 Jul 31. PMID: 28774773.

45 M. Klinke, D. Vincent, M. Trochimiuk, B. Appl, B. Tiemann, R. Bergholz, *et al.*, Degradation of Extracellular DNA Significantly Ameliorates Necrotizing Enterocolitis Severity in Mice, *J. Surg. Res.*, 2019, **235**, 513–520, DOI: **10.1016/j.jss.2018.10.041**. Epub 2018 Nov 26. PMID: 30691836.

46 M. Jiménez-Alcázar, C. Rangaswamy, R. Panda, J. Bitterling, Y. J. Simsek, A. T. Long, *et al.*, Host DNases prevent vascular occlusion by neutrophil extracellular traps, *Science*, 2017, **358**(6367), 1202–1206, DOI: **10.1126/science.aam8897**. PMID: 29191910.

47 C. J. Bean, S. L. Boulet, D. Ellingsen, M. E. Pyle, E. A. Barron-Casella, J. F. Casella, *et al.*, Heme oxygenase-1 gene promoter polymorphism is associated with reduced incidence of acute chest syndrome among children with sickle cell disease, *Blood*, 2012, **120**(18), 3822–3828, DOI: **10.1182/blood-2011-06-361642**. Epub 2012 Sep 10. PMID: 22966170; PMCID: PMC3488892.

48 T. Islam, R. McConnell, W. J. Gauderman, E. Avol, J. M. Peters and F. D. Gilliland, Ozone, oxidant defense genes, and risk of asthma during adolescence, *Am. J. Respir. Crit. Care Med.*, 2008, **177**(4), 388–395, DOI: **10.1164/rccm.200706-863OC**. Epub 2007 Nov 29. PMID: 18048809; PMCID: PMC2258440.

49 B. Liu, J. Wang and Z. Ren, SKP2-Promoted Ubiquitination of FOXO3 Promotes the Development of Asthma, *J. Immunol.*, 2021, **206**(10), 2366–2375, DOI: **10.4049/jimmunol.2000387**. Epub 2021 Apr 9. PMID: 33837090.

50 W. Thijs, K. Janssen, A. M. van Schadewijk, S. E. Papapoulos, S. le Cessie, S. Middeldorp, *et al.*, Nasal Levels of Antimicrobial Peptides in Allergic Asthma Patients and Healthy Controls: Differences and Effect of a Short 1,25(OH)2 Vitamin D3 Treatment, *PLoS One*, 2015, **10**(11), e0140986, DOI: **10.1371/journal.pone.0140986**. PMID: 26545199; PMCID: PMC4636236.

51 F. Roth-Walter, R. Schmutz, N. Mothes-Luksch, P. Lemell, P. Zieglmayer, R. Zieglmayer, *et al.*, Clinical efficacy of sublingual immunotherapy is associated with restoration of steady-state serum lipocalin 2 after SLIT: a pilot study, *World Allergy Organ. J.*, 2018, **11**(1), 21, DOI: **10.1186/s40413-018-0201-8**. PMID: 30323863; PMCID: PMC6166283.

52 J. Jian, S. Li, N. Fang, Y. Z. Cao, L. Zhen, J. B. Qin, *et al.*, Pim-3 alleviates lipopolysaccharide-stimulated AR42J pancreatic acinar cell injury via improving the inflammatory microenvironment, *Exp. Ther. Med.*, 2019, **18**(6), 4427–4435, DOI: **10.3892/etm.2019.8094**. Epub 2019 Oct 10. PMID: 31777546; PMCID: PMC6862483.

53 M. Wang, S. Tang, X. Yang, X. Xie, Y. Luo, S. He, *et al.*, Identification of key genes and pathways in chronic rhinosinusitis with nasal polyps and asthma comorbidity using bioinformatics approaches, *Front. Immunol.*, 2022, **13**, 941547, DOI: **10.3389/fimmu.2022.941547**. PMID: 36059464; PMCID: PMC9428751.

54 P. V. Tomazic, R. Birner-Gruenberger, A. Leitner, S. Spoerk and D. Lang-Loidolt, Seasonal proteome changes of nasal mucus reflect perennial inflammatory response and reduced defence mechanisms and plasticity in allergic rhinitis, *J. Proteomics*, 2016, **133**, 153–160, DOI: **10.1016/j.jprot.2015.12.021**. Epub 2015 Dec 28. PMID: 26732727.

55 K. Skrzypczak, W. Gustaw, D. Szwajgier, E. Fornal and A. Waśko, κ-Casein as a source of short-chain bioactive peptides generated by Lactobacillus helveticus, *J. Food Sci. Technol.*, 2017, **54**(11), 3679–3688, DOI: **10.1007/s13197-017-2830-2**. Epub 2017 Sep 12. PMID: 29051663; PMCID: PMC5629177.

56 M. Yamashita, M. Miyoshi, M. Iwai, R. Takeda, T. Ono and T. Kabuki, Lactobacillus helveticus SBT2171 Alleviates Perennial Allergic Rhinitis in Japanese Adults by Suppressing Eosinophils: A Randomized, Double-Blind, Placebo-Controlled Study, *Nutrients*, 2020, **12**(12), 3620, DOI: **10.3390/nu12123620**. PMID: 33255731; PMCID: PMC7760906.

57 Z. Zhu, C. C. Jr, Y. Raita, M. Fujiogi, L. Liang, E. P. Rhee, *et al.*, Metabolome subtyping of severe bronchiolitis in infancy and risk of childhood asthma, *J. Allergy Clin. Immunol.*, 2022, **149**(1), 102–112, DOI: **10.1016/j.jaci.2021.05.036**. Epub 2021 Jun 10. PMID: 34119532; PMCID: PMC8660920.

58 M. Tuzova, J. C. Jean, R. P. Hughey, L. A. Brown, W. W. Cruikshank, J. Hiratake, *et al.*, Inhibiting lung lining fluid glutathione metabolism with GGsTop as a novel treatment for asthma, *Front. Pharmacol.*, 2014, **5**, 179, DOI:

10.3389/fphar.2014.00179. PMID: 25132819; PMCID: PMC4116799.

59 Y. Fan, C. Yang, J. Zhou, X. Cheng, Y. Dong, Q. Wang, *et al.*, Regulatory effect of glutathione on treg/Th17 cell balance in allergic rhinitis patients through inhibiting intracellular autophagy, *Immunopharmacol. Immunotoxicol.*, 2021, **43**(1), 58–67, DOI: 10.1080/08923973.2020.1850762. Epub 2020 Dec 7. PMID: 33285073.

60 Y. Shan, J. Li, A. Zhu, W. Kong, R. Ying and W. Zhu, Ginsenoside Rg3 ameliorates acute pancreatitis by activating the NRF2/HO-1-mediated ferroptosis pathway, *Int. J. Mol. Med.*, 2022, **50**(1), 89, DOI: 10.3892/ijmm.2022.5144. Epub 2022 May 18. PMID: 35582998; PMCID: PMC9162051.

61 D. Fussbroich, K. Zimmermann, A. Göpel, O. Eickmeier, J. Trischler, S. Zielen, *et al.*, A specific combined long-chain polyunsaturated fatty acid supplementation reverses fatty acid profile alterations in a mouse model of chronic asthma, *Lipids Health Dis.*, 2019, **18**(1), 16, DOI: 10.1186/s12944-018-0947-6. PMID: 30658644; PMCID: PMC6339374.

62 H. H. Chang, C. S. Chen and J. Y. Lin, Dietary perilla oil lowers serum lipids and ovalbumin-specific IgG1, but increases total IgE levels in ovalbumin-challenged mice, *Food Chem. Toxicol.*, 2009, **47**(4), 848–854, DOI: 10.1016/j.fct.2009.01.017. PMID: 19271319.

63 F. H. Chilton, F. J. Averill, W. C. Hubbard, A. N. Fonteh, M. Triggiani and M. C. Liu, Antigen-induced generation of lyso-phospholipids in human airways, *J. Exp. Med.*, 1996, **183**(5), 2235–2245, DOI: 10.1084/jem.183.5.2235. PMID: 8642333; PMCID: PMC2192563.

64 J. Scholz, J. Kuhrau, F. Heinrich, G. A. Heinz, A. Hutloff, M. Worm, *et al.*, Vitamin A controls the allergic response through T follicular helper cell as well as plasmablast differentiation, *Allergy*, 2021, **76**(4), 1109–1122, DOI: 10.1111/all.14581. Epub 2020 Sep 20. PMID: 32895937.

65 L. Feng, F. Sun, Y. Chen, S. S. Athari and X. Chen, Studying the Effects of Vitamin A on the Severity of Allergic Rhinitis and Asthma, *Iran. J. Allergy, Asthma Immunol.*, 2021, **20**(6), 648–692, DOI: 10.18502/ijaai.v20i6.8018. PMID: 34920650.

66 M. A. Shaheen, M. A. Mahmoud, M. M. Abdel Aziz, H. I. El Morsy and K. A. Abdel Khalik, Sputum dipalmitoylphosphatidylcholine level as a novel airway inflammatory marker in asthmatic children, *Clin. Respir. J.*, 2009, **3**(2), 95–101, DOI: 10.1111/j.1752-699X.2009.00127.x. PMID: 20298384.

67 W. Zhang, R. Tang, G. Ba, M. Li and H. Lin, Anti-allergic and anti-inflammatory effects of resveratrol via inhibiting TXNIP-oxidative stress pathway in a mouse model of allergic rhinitis, *World Allergy Organ. J.*, 2020, **13**(10), 100473, DOI: 10.1016/j.waojou.2020.100473. PMID: 33133334; PMCID: PMC7586246.

68 S. R. McSweeney, E. Warabi and R. C. Siow, Nrf2 as an Endothelial Mechanosensitive Transcription Factor: Going With the Flow, *Hypertension*, 2016, **67**(1), 20–29, DOI: 10.1161/HYPERTENSIONAHA.115.06146. Epub 2015 Nov 23. PMID: 26597822.

69 P. Ye, X. L. Yang, X. Chen and C. Shi, Hyperoside attenuates OVA-induced allergic airway inflammation by activating Nrf2, *Int. Immunopharmacol.*, 2017, **44**, 168–173, DOI: 10.1016/j.intimp.2017.01.003. PMID: 28107754.

70 Y. Sahoyama, F. Hamazato, M. Shiozawa, T. Nakagawa, W. Suda, Y. Ogata, *et al.*, Multiple nutritional and gut microbial factors associated with allergic rhinitis: the Hitachi Health Study, *Sci. Rep.*, 2022, **12**(1), 3359, DOI: 10.1038/s41598-022-07398-8. PMID: 35233003; PMCID: PMC8888718.

71 M. O. Dillioglugil, H. Maral Kir, M. D. Gulkac, A. Ozon Kanli, H. K. Ozdogan, O. Acar, *et al.*, Protective effects of increasing vitamin E and a doses on cisplatin-induced oxidative damage to kidney tissue in rats, *Urol. Int.*, 2005, **75**(4), 340–344, DOI: 10.1159/000089171. PMID: 16327303.

72 M. Navidhamidi, A. Nazari, S. Dehghan, A. Ebrahimpour, R. Nasrnezhad and F. Pourabdolhossein, Therapeutic Potential of Combined Therapy of Vitamin A and Vitamin C in the Experimental Autoimmune Encephalomyelitis (EAE) in Lewis Rats, *Mol. Neurobiol.*, 2022, **59**(4), 2328–2347, DOI: 10.1007/s12035-022-02755-0. Epub 2022 Jan 24. PMID: 35072933.

73 X. Zhu, B. Wang, X. Zhang, X. Chen, J. Zhu, Y. Zou, *et al.*, Alpha-linolenic acid protects against lipopolysaccharide-induced acute lung injury through anti-inflammatory and anti-oxidative pathways, *Microb. Pathog.*, 2020, **142**, 104077, DOI: 10.1016/j.micpath.2020.104077. Epub ahead of print. PMID: 32084579.

74 S. I. Alam, M. W. Kim, F. A. Shah, K. Saeed, R. Ullah and M. O. Kim, Alpha-Linolenic Acid Impedes Cadmium-Induced Oxidative Stress, Neuroinflammation, and Neurodegeneration in Mouse Brain, *Cells*, 2021, **10**(9), 2274, DOI: 10.3390/cells10092274. PMID: 34571925; PMCID: PMC8467071.

75 J. Zhao, I. Endoh, K. Hsu, N. Tedla, Y. Endoh and C. L. Geczy, S100A8 modulates mast cell function and suppresses eosinophil migration in acute asthma, *Antioxid. Redox Signal.*, 2011, **14**(9), 1589–1600, DOI: 10.1089/ars.2010.3583. Epub 2011 Feb 28. PMID: 21142608.

76 M. Zou, X. Su, L. Wang, X. Yi, Y. Qiu, X. Yin, *et al.*, The Molecular Mechanism of Multiple Organ Dysfunction and Targeted Intervention of COVID-19 Based on Time-Order Transcriptomic Analysis, *Front. Immunol.*, 2021, **12**, 729776, DOI: 10.3389/fimmu.2021.729776. PMID: 34504502; PMCID: PMC8421734.

77 K. Kang, F. Xie, J. Mao, Y. Bai and X. Wang, Significance of Tumor Mutation Burden in Immune Infiltration and Prognosis in Cutaneous Melanoma, *Front. Oncol.*, 2020, **10**, 573141, DOI: 10.3389/fonc.2020.573141. PMID: 33072607; PMCID: PMC7531222.

78 W. Wu, M. Wang, C. Li, Z. Zhu, Y. Zhang, D. Wu, *et al.*, LncRNA Snhg1 Plays an Important Role via Sequestering rno-miR-139-5p to Function as a ceRNA in Acute Rejection After Rat Liver Transplantation Based on the Bioinformatics Analysis, *Front. Genet.*, 2022, **13**, 827193, DOI: 10.3389/fgene.2022.827193. PMID: 35719364; PMCID: PMC9203122.

79 X. Fei, H. Hu, Y. Luo, Q. Shi and A. Wei, Widely targeted metabolomic profiling combined with transcriptome analysis provides new insights into amino acid biosynthesis in green and red pepper fruits, *Food Res. Int.*, 2022, **160**, 111718, DOI: **10.1016/j.foodres.2022.111718**. Epub 2022 Jul 22. PMID: 36076459.

80 M. Lian, Y. Tao, J. Chen, X. Shen, L. Hou, S. Cao, *et al.*, Variation of PPARG Expression in Chemotherapy-Sensitive Patients of Hypopharyngeal Squamous Cell Carcinoma, *PPAR Res.*, 2021, **2021**, 5525091, DOI: **10.1155/2021/5525091**. PMID: 34054937; PMCID: PMC8149230.

81 Y. Zheng, B. Qi, W. Gao, Z. Qi, Y. Liu, Y. Wang, *et al.*, Macrophages-Related Genes Biomarkers in the Deterioration of Atherosclerosis, *Front. Cardiovasc. Med.*, 2022, **9**, 890321, DOI: **10.3389/fcvm.2022.890321**. PMID: 35845072; PMCID: PMC9282674.

82 P. Shannon, A. Markiel, O. Ozier, N. S. Baliga, J. T. Wang, D. Ramage, *et al.*, Cytoscape: a software environment for integrated models of biomolecular interaction networks, *Genome Res.*, 2003, **13**(11), 2498–2504, DOI: **10.1101/gr.1239303**. PMID: 14597658; PMCID: PMC403769.

83 Z. Pang, J. Chong, G. Zhou, D. A. de Lima Morais, L. Chang, M. Barrette, *et al.*, MetaboAnalyst 5.0: narrowing the gap between raw spectra and functional insights, *Nucleic Acids Res.*, 2021, **49**(W1), W388–W396, DOI: **10.1093/nar/gkab382**. PMID: 34019663; PMCID: PMC8265181.